Quantum annealing via real-time Schrödinger dynamics

Òscar Boyle García
Facultat de Física, Universitat de Barcelona, Diagonal 645, 08028 Barcelona, Spain.

Advisor: Matteo Palassini

Abstract: Quantum annealing provides a way to potentially solve optimisation problems faster than its classical counterpart, simulated annealing, but the suitability of this method is still open to debate. Here we present an example of simulated quantum annealing of a 2D Ising spin glass model by the real-time evolution governed by the Schrödinger equation. A bias towards certain ground states is observed for larger annealing times. The final states are compatible with the results obtained in a previous study using path-integral Monte Carlo for simulated quantum annealing.

I. INTRODUCTION

The interest in solving optimisation problems has been renewed by advances in quantum computation. In particular, NP-complete problems have been an important field of study in computational sciences, as there are no current efficient classical algorithms to solve them in polynomial time. The importance of these problems lies in the ability to map one to another—if we can solve one in polynomial time we can solve them all. One of these is the spin glass model, a condensed matter system that has been an important area of study in the field of statistical mechanics. It is typically described using the Ising model, which arranges the magnetic dipole moments of atoms (spins) in a lattice, these take a value of ± 1 and interact with their neighbours. The interactions of a spin glass have random sign, introducing properties like frustration and meta-stable minima which give great complexity to the problem.

A way to study these problems is by the method of stochastic optimisation known as classical simulated annealing (CSA), which finds approximate global solutions of a system described by a cost-function $\hat{\mathcal{H}}(x)$ by introducing variable thermal fluctuations (either real or fictitious). By introducing large fluctuations, i.e. large temperature, the system can surpass the barriers between meta-stable minima and explore the whole configuration space. Then, by reducing the temperature during a sufficiently slow annealing time τ, we obtain the minimum energy at $T = 0$. Using quantum mechanics, we can follow an analogous process. Instead of thermal fluctuations, we provide the necessary quantum fluctuations for the system described by $\Psi(x,t)$ to explore all the possible states by means of quantum tunnelling. Overtime, we reduce the strength of these fluctuations in order to localise $\Psi(x,t)$ at the lowest possible energy. This method, called quantum annealing (QA), has already been implemented experimentally by using quantum computers[1], even for commercial use with the introduction of the D-wave quantum annealers [2]. Some experiments have shown faster convergence compared to CSA[3]. On the other hand, there have also been studies that show an intrinsic bias for certain ground states (GS) of the studied problem, both simulated and experimental[5][4]. It is still a matter of debate whether QA is a suitable method for optimisation, as an ideal algorithm should explore all possible solutions with equal probability.

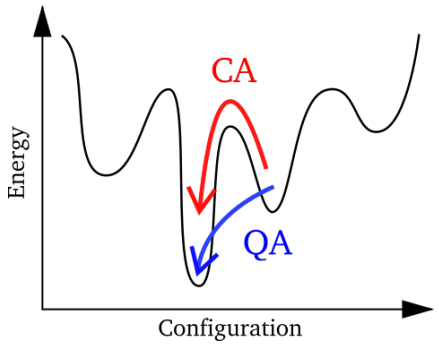

FIG. 1: Representation of simulated annealing and quantum annealing methods for finding minimum energy in configuration space

One way of simulating QA on a classical computer is by the real-time evolution (RTE-SQA) of the system using Schrödinger's equation. This allows us to observe the convergence for different annealing times following the quantum dynamics. In our case we will consider a 2D Ising spin glass model of size $N = 16$. Computing the real-time evolution of these systems is quite time consuming, for this reason only a few studies have been made with similar sized problems[6][7].

Another way to study these systems is by using path-integral Monte Carlo (PIMC-SQA), a statistical sampling method. This method does not involve any dynamics of the system, instead it uses an imaginary time to obtain its results. By using PIMC one has access to larger systems using the same computational power. We will be comparing our results with those of a previous work carried out by another student [8] in Sec. IV. These methods are based on completely different dynamics and are therefore complementary, not interchangeable.

In the following sections we will be discussing the RTE of a spin glass. In Sec. II we will present the problem of QA of the 2D Ising spin glass model, with a brief description of the computations given in Sec. III. Finally, the numerical results are shown in Sec. IV and discussed

further in Sec. V.

II. QUANTUM ANNEALING OF A SPIN GLASS

To solve an optimisation problem using quantum annealing, we consider a classical Hamiltonian $\mathcal{H}_0$, the cost-energy function whose ground states correspond to the solution we are trying to obtain. As mentioned before, a typical example of $\mathcal{H}_0$ is the two-dimensional Ising spin glass Hamiltonian:

$$\hat{\mathcal{H}}_0 = -\sum_{\langle i,j \rangle} J_{ij} \hat{\sigma}_i^z \hat{\sigma}_j^z, \tag{1}$$

where the interaction is governed by the random coupling J_{ij} between two nearest neighbour spins ($\sigma_i = \pm 1$). To minimise $\mathcal{H}_0$ we must choose an adequate quantum basis in which $\hat{\mathcal{H}}_0$ is diagonal. For the quantum fluctuations, we consider the interaction of the spins with a transverse field given by $\hat{\mathcal{H}}_1 = \sum_{i=1}^{N} \hat{\sigma}_i^x$. Finally, we introduce the time-dependant Hamiltonian as:

$$\hat{\mathcal{H}}(t) = \hat{\mathcal{H}}_0 - \Gamma(t)\hat{\mathcal{H}}_1, \tag{2}$$

where $\Gamma(t)$ satisfies $\Gamma(0) \to \infty$ and $\Gamma(t \to \infty) \to 0$ (In our case the final time is τ), and $\hat{\mathcal{H}}_0$ is shown in Eq. 1. This way, the quantum fluctuations allow the system to explore all the possible states at initial time $t = 0$ and slowly evolve untill $\hat{\mathcal{H}}(\tau) = \hat{\mathcal{H}}_0$. For simplicity we consider $\Gamma(t) = \Gamma_0(1 - t/\tau)$, where Γ_0 is a finite value that dictates the initial strength of the transverse field Hamiltonian. For the purposes of this paper a value of $\Gamma_0 = 3$ will suffice in order to replicate the real quantum annealers that use $\Gamma_0 \to \infty$.

Following the principle of quantum mechanics the real-time evolution of the state is governed by Schrödinger's equation:

$$\begin{aligned} i\frac{d}{dt}\left|\Psi(t)\right\rangle &= \hat{\mathcal{H}}(t)\left|\Psi(t)\right\rangle \\ \hat{\mathcal{H}}(0)\left|\Psi(0)\right\rangle &= \epsilon_{gs}\left|\Psi(0)\right\rangle \end{aligned} \tag{3}$$

where $\hbar = 1$ and ϵ_{gs} is the eigenvalue of the initial Hamiltonian, so the initial state considered is the GS of $\mathcal{H}(0)$.

If the annealing time τ is large enough, therefore satisfying the adiabatic theorem[9], the final state will be the ground state of $\hat{\mathcal{H}}(\tau) = \hat{\mathcal{H}}_0$. It is important to describe the energy spectrum of this problem. At time $t = 0$, we obtain a large amount of eigenvalues of $\hat{\mathcal{H}}(0)$ and ss we evolve the system we will observe a multitude of energy bands. These describe the energy variation of the system starting at the initial eigenvalues and converging at the degenerate eigenvalues of $\hat{\mathcal{H}}_0$. If the QA (or SQA) is infinitely slow during evolution process, the system will follow the minimum energy, defined by $E_0(t)$, which is the lowest value of the CGS energy band. We also need to define the the minimum value $E_1(t)$ of the first excited state (FES) band. These two bands never cross but do get close to each other at a certain $\Gamma(t)$, this is described as the Landau Zenner avoided crossings. The probability of the system evolving as a ground state is heavily influenced by this minimum gap between $E_0(t)$ and $E_1(t)$ defined as $\Delta_{min} = min_{\Gamma(t)}(E_1(t) - E_0(t))$. The non-adiabatic transition probability between these two bands, given by the Landau-Zener formula [10], increases as Δ_{min} decreases. This energy gap will dictate the complexity of a problem and the time required to solve it.

We will consider a two-dimensional lattice of size $N = L \times L$, with periodic boundary conditions in which we will study the spin glass, with $\hat{\mathcal{H}}_0$ shown in Eq. 1. We will study the $\pm J$ model, in which the distribution of these interactions is described by:

$$P(J_{ij}) = p\delta(J_{ij} - J) + (1 - p)\delta(J_{ij} + J), \tag{4}$$

where δ is Dirac delta function, $J = 1$ and $p = 0.5$ so we get equal probability. This model results in a highly degenerate spin glass with an exponential number of CGS.

We will consider the computational basis $\{|x\rangle\}$ of the system, consisting of all the possible configurations of spins (2^N elements). In this basis, we can write the state $|\Psi(t)\rangle$ as:

$$\left|\Psi(t)\right\rangle = \sum_x c_x \left|x\right\rangle. \tag{5}$$

This will give us a diagonal Hamiltonian $\hat{\mathcal{H}}_0$ with every element equal to the classical energy of its corresponding configuration, the minimum energy states of the classical Hamiltonian $\mathcal{H}$ are defined as the classical ground states (CGS). The non-diagonal matrix $\langle x|\,\hat{\mathcal{H}}_1(t)\,|y\rangle$ will be mostly empty except for values equal to $-\Gamma(t)$ for connected states. Two states $|x\rangle$ and $|x'\rangle$ are connected if one can obtain the other by the flip of one spin. In particular we will choose the states in lexicographical order, assigning a 1 and 0 to each +1 and -1 spin respectively and reading the binary number as the i.d. of each configuration of spins.

III. NUMERICAL ANALYSIS

In order to obtain numerical values for the evolution of the system we will be using a Runge Kutta 4^{th} order method (RK4) to solve the Schrödinger equation:

$$i\frac{d}{dt}c_y(t) = \sum_x \hat{\mathcal{H}}_{xy}(t)c_x(t) \tag{6}$$

The initial state given by $c_x(0)$ is obtained by diagonalizing $\hat{\mathcal{H}}(0)$, and we compute $\hat{\mathcal{H}}(t)$ at each time t by altering only the non-zero elements of $\hat{\mathcal{H}}_1$.

Each element consists of a real and imaginary element so we will have to compute 2^{N+1} coupled equations $N_{steps} = (\tau/\Delta)$ times, where we have defined the time

step Δ as the variation of time $(t_{n+1} - t_n)$ for each iteration n. Therein lies the difficulty of obtaining results for the real-time evolution of large systems. To avoid unnecessary floating-point operations we will use the fact that the time-dependant Hamiltonian is a sparse matrix: the only non-zero elements for each row correspond to the diagonal value and the N connected states. This reduces the scaling of our calculations from $2^N \times 2^N$ to $N \times 2^N$.

The following results were obtained using a step $\Delta = 10^{-2}$ for a $L = 4$ system, $N = 16$ spins.

IV. NUMERICAL RESULTS

We solved for 100 different instances $\mathcal{I}$ with randomly generated couplings J_{ij}, evolving them for different annealing times τ. For each $\mathcal{I}$ we computed the values of the c_x coefficients and the evolution of the expected value of the energy $\langle\hat{\mathcal{H}}(t)\rangle = \langle\Psi(t)|\,\hat{\mathcal{H}}(t)\,|\Psi(t)\rangle$. Using the exact minimum eigenvalue of $\hat{\mathcal{H}}(t)$, $E_0(\Gamma(t))$, we can check the convergence of our results by defining the residual energy as:

$$E_{res}(t) = E_0(\Gamma(t)) - \langle\hat{\mathcal{H}}(t)\rangle, \tag{7}$$

In Fig.2 we show how a larger annealing time reduces the final residual energy. The slight deviation for the values of the average $E_{res}(t)$ as $\Gamma \to 0$ is due to some excited states still being occupied.

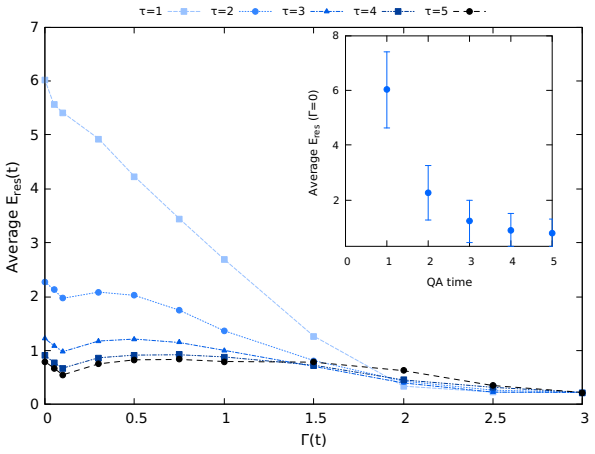

FIG. 2: Evolution of energy as Γ tends to zero. The inset figure shows the final average residual time for each τ.

To study the successful convergence of a certain $\mathcal{I}$ we define the probability of success P_{succ} as the probability of obtaining a CGS as the final state, *i.e.*:

$$P_{succ} = \frac{\sum_{GS} |c_x|^2}{\sum |c_x|^2}. \tag{8}$$

Here, the top sum is over the CGS and the bottom sum is over all configurations in the computational basis.

If τ is too big or too small we get $(P_{succ} \to 1)$ or $(P_{succ} \to 0)\,\forall\,\mathcal{I}$ respectively, as shown in Fig.3.

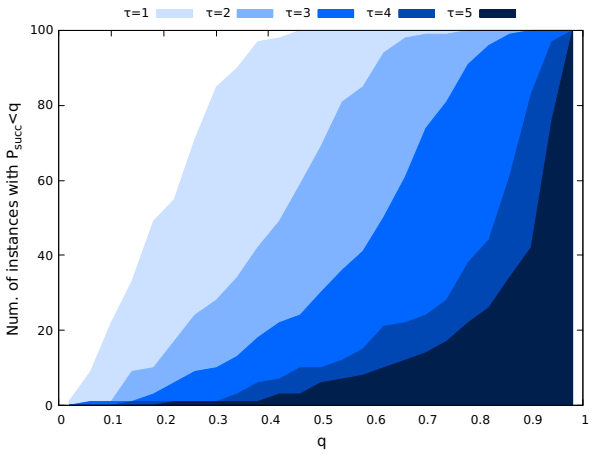

FIG. 3: Cumulative distribution of P_{succ} for different annealing times.

We considered $\tau = 2$ as a good half-way point between the two extremes so we get a broad distribution of different P_{succ} between 0 and 1. For these values, we can compute the minimum gap between the GS and FES Δ_{min} by the exact diagonalization of $\hat{\mathcal{H}}(t)$ for a certain time t. Fig. 4 shows the correlation predicted by the Landau-Zener theory: as the gap increases, the chances of a non-adiabatic transition drop, so the evolution is more likely to converge at a CGS. No relation was found between the value of Γ at which the gap is minimum and P_{succ}. We also compared the values of P_{succ} with those

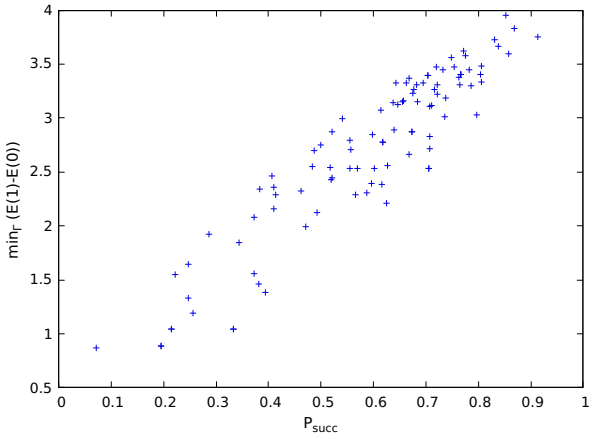

FIG. 4: Success probability vs Δ_{min} for a QA time $\tau = 2$.

obtained using PIMC[8], for which the same $\mathcal{I}$ have been used. In Fig. 5 we see a good indication of the validity of the results obtained with our method. The discrepancies are due to the annealing time not being exactly the same (the annealing time of the PIMC method is given in number of Monte Carlo steps), as the RTE method is not trivially related to PIMC, but overall the results seem to be in agreement. Further analysis shows this in more detail.

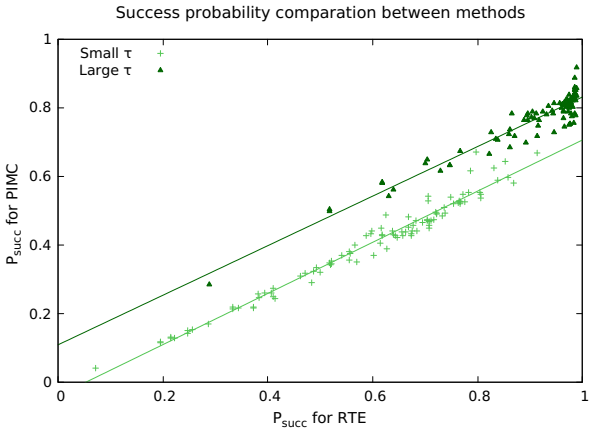

FIG. 5: Comparison between success probabilities for PIMC and real-time evolution. Two different annealing times have been used. For RTE we used $\tau = 2$ and $\tau = 5$. For PIMC the times correspond 30 and 200 monte carlo steps.

It is also important to discuss the distribution of ground states. The effectiveness of a method for solving optimisation problems greatly depends on its ability to explore every solution equally. In an adiabatic evolution of $\hat{\mathcal{H}}(t)$ we would expect to visit every CGS with equall probability but our results show a deviation from the uniform distribution as the annealing time τ increases. An example of this behaviour is seen in Fig.6 for an instance with 76 CGS. A certain symmetry is observed in this figure. This is due to the order of the CGS, which is lexicographical. In this order, the first and last CGS are equivalent configurations with all the spins flipped, the second and second last CGS are also equivalent, and so on. To quantify this non-uniformity we considered

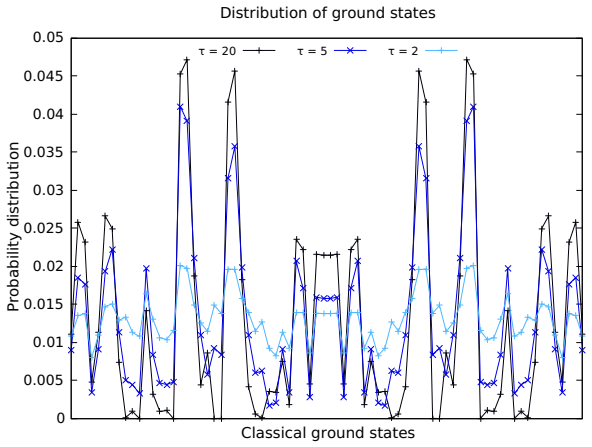

FIG. 6: GS distribution for different annealing times.

the inverse participation ratio (IPR) which will give us a qualitative behaviour of the CGS distribution. The IPR can be defined as:

$$\text{IPR} = \frac{P_{succ}^2}{\sum_{CGS} p_x^2} \tag{9}$$

For a uniform distribution, $p_x = 1/N_{CGS}$, we obtain a the linear relation IPR$= N_{CGS}$, where N_{CGS} is the number of CGS. If the probability of some CGS dominates over others, the slope of this relation between IPR and N_{CGS} decreases, with the lower limit being 1 for a completely non-uniform distribution corresponding to just one CGS $|x_0\rangle$, for which $p_x = \delta_{x,x_0}$ where δ_{x,x_0} is the Kronecker delta. Using the different annealing times we plotted these values as a function of N_{CGS} so that the most uniform distributions behave like $y = x$ and as we lose uniformity the slope decreases. These results are shown in Fig. 7. We see a deviation from the uniform distribution of CGS as we increase the annealing time. The non-uniformity of the CGS distribution is also com-

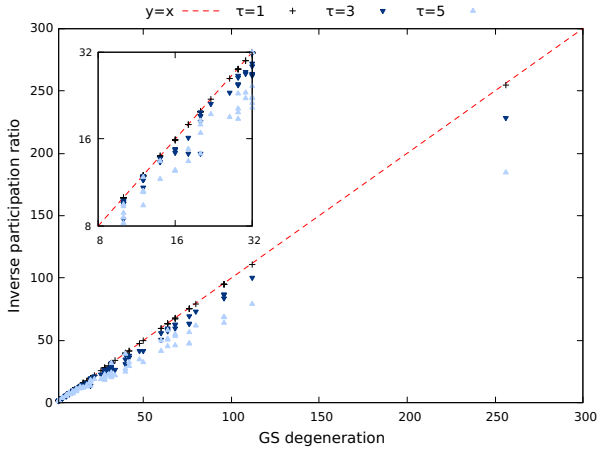

FIG. 7: IPR vs N_G for different annealing times.

patible with the results obtained by PIMC. Using the same instance as before we can observe in Fig.8 the similarities between both methods. Once again, we do not have a direct correspondence with the annealing times, which causes some discrepancies. Still, the CGS are visited similarly for both computations so the biases are a result of intrinsic properties of the spin glass and not due to the method used.

We also computed the values of the IPR for this method, presented in Fig.9. For small annealing times both methods explore all GS in a relatively uniform manner, resulting in a very strong correlation between results. Increasing the QA time introduces some discrepancies to the results.

V. CONCLUSIONS AND COMMENTARY

We were able to successfully perform the QA of a spin glass using Schrödinger's equation for real-time evolution. In doing so, we observed the correlation between

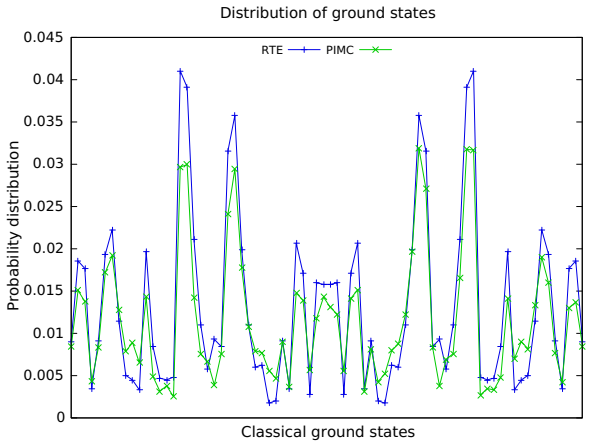

FIG. 8: GS distribution for the two methods. For RTE $\tau = 5$. For

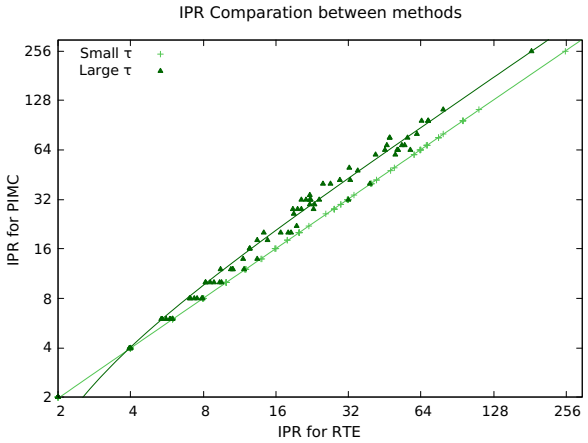

FIG. 9: Probability of each GS for two different annealing times. The annealing times for RTE correspond to $\tau = 2$ and $\tau = 5$. and for PIMC the times correspond 30 and 200 Monte Carlo steps.

the success of a QA and the minimum gap between energy bands Δ_{min}, described by the Landau-Zener theory. We were also able to verify the results obtained by PIMC, showing a good correlation between the two independent methods. It would be interesting for future studies to analyse the behaviour of the clusters of states and their entropy —two states are in the same cluster if they are connected by a path of constant energy by single flip spins. [8]

As for the results concerning the non-uniformity of the CGS distribution, it is important to analyse the initial conditions of the problem. The initial quantum ground state (QGS) obtained by diagonalizing the time-dependent Hamiltonian would ideally equally explore all the states of the spin glass. For a finite Γ_0 we still obtain equal probabilities for CGS due to a superposition of these states in the QGS. This explains why smaller annealing times return more uniform distributions. As we increase the annealing time some CGS are visited with more frequency than others, resulting in peaks in their probability. Future research of this behaviour is needed for determinate conclusions but this phenomena appears to be intrinsic to each instance, likely linked to the energy spectrum of the states. A method for optimisation that misses certain solutions is not ideal so we have yet to see if QA is a suitable approach to solve these kinds of problems.

Acknowledgments

I would like to thank Dr. Matteo Palassini for all the advice and patience during these trying times. Secondly, the results presented here would have not been possible without Álvaro Borrás, who performed the PIMC-SQA in his own TFG. Finally, i would also like to thank my friends and family for their support during all these years, specially these last few months.

[1] Perdomo-Ortiz, A., Fluegemann, J., Narasimhan, S. et al. "A quantum annealing approach for fault detection and diagnosis of graph-based systems." Eur. Phys. J. Spec. Top. 224, 131–148 (2015).

[2] D-Wave Systems Inc. http://www.dwavesys.com.

[3] Brooke, J., D. Bitko, and G. Aeppli. "Quantum annealing of a disordered magnet." Science 284.5415 (1999): 779-781.

[4] Mandra, Salvatore, Zheng Zhu, and Helmut G. Katzgraber. "Exponentially biased ground-state sampling of quantum annealing machines with transverse-field driving hamiltonians." Physical review letters 118.7 (2017): 070502.

[5] Matsuda, Yoshiki, Hidetoshi Nishimori, and Helmut G. Katzgraber. "Ground-state statistics from annealing algorithms: quantum versus classical approaches." New Journal of Physics 11.7 (2009): 073021.

[6] Farhi, Edward, et al. "A quantum adiabatic evolution algorithm applied to random instances of an NP-complete problem." Science 292.5516 (2001): 472-475.

[7] Kadowaki, Tadashi, and Hidetoshi Nishimori. "Quantum annealing in the transverse Ising model." Physical Review E 58.5 (1998): 5355.

[8] Álvaro Borrás. "Simulated Quantum Annealing of a spin glass". Universitat de Barcelona (2019)

[9] Messiah, Albert. *Quantum mechanics*. Vol. 2. Elsevier, 1981.

[10] Landau L D and Lifshitz E M 2003 *Quantum mechanics: non-relativistic theory*, 3rd ed (Butterworth-Heinemann)